

AperTO - Archivio Istituzionale Open Access dell'Università di Torino

An eco-epidemiological model supporting rational disease management of *Xylella fastidiosa*. An application to the outbreak in Apulia (Italy)

This is the author's manuscript

Original Citation:

Availability:

This version is available <http://hdl.handle.net/2318/1890659> since 2023-02-06T13:16:23Z

Published version:

DOI:10.1016/j.ecolmodel.2022.110226

Terms of use:

Open Access

Anyone can freely access the full text of works made available as "Open Access". Works made available under a Creative Commons license can be used according to the terms and conditions of said license. Use of all other works requires consent of the right holder (author or publisher) if not exempted from copyright protection by the applicable law.

(Article begins on next page)

1 **An eco-epidemiological model supporting rational disease management of *Xylella fastidiosa*. An**
2 **application to the outbreak in Apulia (Italy)**

3

4 Gilioli Gianni^a, Simonetto Anna^{a*}, Colturato Michele^a, Bazarra Noelia^b, Fernández José R.^b, Naso
5 Maria Grazia^a, Boscia Donato^c, Bosco Domenico^d, Dongiovanni Crescenza^e, Maiorano Andrea^f,
6 Mosbach-Schulz Olaf^f, Navas Cortés Juan A.^g, Saponari Maria^c

7

8 ^aDipartimento di Ingegneria Civile, Architettura, Territorio e Ambiente e di Matematica, Università
9 di Brescia, Italy

10 ^bDepartamento de Matemática Aplicada I, Universidade de Vigo, ETSI Telecomunicación, Campus
11 As Lagoas Marcosende s/n, Vigo, 36310, Spain

12 ^cConsiglio Nazionale delle Ricerche, Istituto per la Protezione Sostenibile delle Piante, Sede
13 Secondaria di Bari, Italy

14 ^dDipartimento di Scienze Agrarie, Forestali e Alimentari, Università degli Studi di Torino, Largo Paolo
15 Braccini, 2, Grugliasco, 10095, Italy

16 ^eCentro di Ricerca, Sperimentazione e Formazione in Agricoltura Basile Caramia, Locorotondo, Italy

17 ^fEuropean Food Safety Authority, Parma, Italy

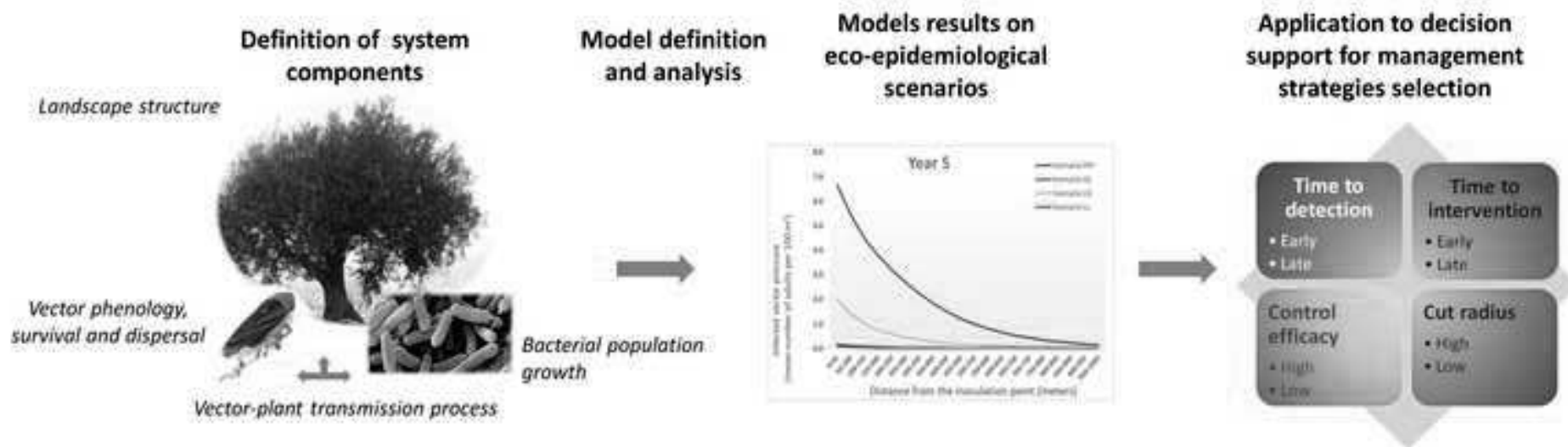
18 ^gInstituto de Agricultura Sostenible (IAS), Consejo Superior de Investigaciones Científicas (CSIC),
19 Avda. Menéndez Pidal s/n, Córdoba, 14004, Spain

20

21 * Corresponding author: Anna Simonetto, anna.simonetto@unibs.it

22

23



Highlights

- *X. fastidiosa* eco-epidemiological model (XEM) describes the continuous spread of Xf
- XEM allows to evaluate different risk reducing options and management practices
- Vector and weed control intervention efficacy resulted as key factors for eradication

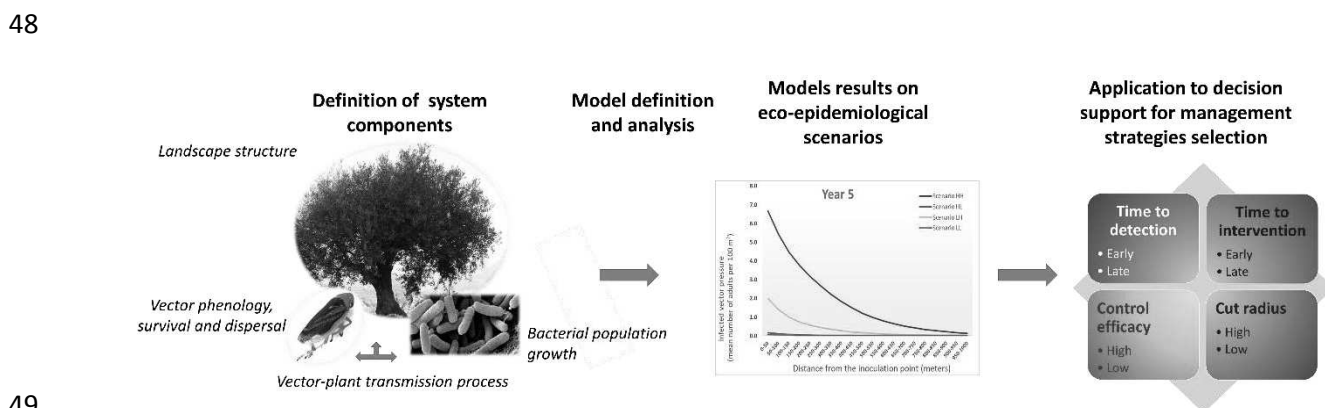
24 **An eco-epidemiological model supporting rational disease management of *Xylella fastidiosa*. An**
25 **application to the outbreak in Apulia (Italy)**

26
27 Abstract

28 Knowledge on the dynamics of *Xylella fastidiosa* infection is an essential element for the effective
29 management of new foci. In this study, we propose an Eco-epidemiological Model (XEM) describing
30 the infection dynamics of *X. fastidiosa* outbreaks. XEM can be applied to design disease
31 management strategies and compare their level of efficacy. XEM is a spatial explicit mechanistic
32 model for short-range spread of *X. fastidiosa* considering: i) the growth of the bacterium in the host
33 plant, ii) the acquisition of the pathogen by the vector and its transmission to host plants, iii) the
34 vector population dynamics, iv) the dispersal of the vector. The model is parametrized based on
35 data acquired on the spread of *X. fastidiosa* subsp. *pauca* in olive groves in the Apulia region. Four
36 epidemiological scenarios were considered combining host susceptibility and vector abundance.
37 Eight management strategies were compared testing several levels of vector control efficacy, plant
38 cutting radius, time to detection and intervention. Simulation results showed that the abundance
39 of the vector is the key factor determining the spread rate of the pathogen. Vector control efficacy
40 and time to detection and intervention emerged as the key factors for an effective eradication
41 strategy. XEM proved to be a suitable tool to support decision making for the drafting and
42 management of emergency plans related to new outbreaks.

43
44 **Keywords:** mechanistic model, short-range spread, olive trees, bacterium, pathosystems,
45 eradication strategies

46
47 Graphical Abstract



51 1. Introduction

52 *Xylella fastidiosa* (*Xf*) is a xylem-limited gram-negative bacterium originating from the Americas,
53 identified in Europe during the last decade when the Italian authorities reported the first outbreak
54 of *Xf* subsp. *pauca* in the south of the Apulia region in 2013. Afterward, the bacterium has also been
55 detected in France (first outbreak in Corse, 2015), Switzerland (detected in 2015, now eradicated),
56 Spain (first outbreak in Balearic islands, 2012), Germany (an isolated infection in 2016 now
57 eradicated), and Portugal (first outbreak in Porto, 2019) (EFSA PLH Panel, 2019; EPPO Reporting
58 Service, 2018, 2019).

59 In Europe, the bacterium represents a significant risk for several crops and therefore a serious
60 threat to food security (EFSA PLH Panel, 2020; Schneider et al., 2020). Host plants, susceptibility and
61 symptoms vary according to the *Xf* subsp./strains (Nunney et al., 2013; Sanderlin, 2017).

62 Several important crop diseases can be associated with *Xf*, such as the Pierce's disease of grapevine,
63 the plum leaf scald, the Citrus variegated chlorosis, the phony peach disease, and as confirmed in
64 Italy, *Xf* is the cause of olive quick decline syndrome, which dramatically brought the Apulia olive
65 growing sector to its knees (Hopkins & Purcell, 2002; Saponari et al., 2017).

66 The bacterium is transmitted by xylem-sap feeding insects (Almeida et al., 2005; Perring et al., 2001;
67 Purcell et al., 1999; Redak et al., 2004). Host species and bacterium strains highly influence vector
68 competence (Cavaliere & Porcelli, 2017; Lopes et al., 2009). In Europe, *Xf* is mainly transmitted by
69 the indigenous vector *Philaenus spumarius* (Cornara et al., 2018; Cruaud et al., 2018; Moralejo et
70 al., 2019). More recently, two other spittlebug species, *Philaenus italosignus* and *Neophilaenus*
71 *campestris*, have also been identified as competent vectors (Cavaliere et al., 2019).

72 The *Xf* epidemiological system is characterized by high variability and heterogeneity according to
73 prevalence and spread of the infection (Sicard et al. 2018; EFSA PLH Panel 2019). The spatial and
74 temporal patterns of disease dynamics strictly depend on the interactions among bacteria, vectors,
75 and host plants in the pathosystem. These interactions are mediated by complex physiological and
76 pathological processes and strongly influenced by environmental variables (e.g., temperature,
77 water stress) (Almeida et al., 2005; Cornara et al., 2017; Jeger and Bragard 2019).

78 Several models have been proposed to investigate the key factors determining the *Xf* dynamics and
79 how to manipulate them to support disease management (Parnell et al., 2017). Focusing on process-
80 based models, a wide variety of approaches can be found in the literature: reaction-diffusion models
81 (Chapman et al., 2015), susceptible-exposed-infectious-removed (SEIR) models (Jeger & Bragard,
82 2019; S. M. White et al., 2020), lattice susceptible, infected, removed (SIR) models (Fierro et al.,

83 2019), spatially-explicit simulation models, short-distance deterministic and long-distance
84 stochastic kernels (S. M. White et al., 2017), discrete-time versions of standard differential
85 equations used in epidemiological compartmental models (S. White et al., 2019), and ordinary
86 differential equation systems (Brunetti et al., 2020). Despite the variety of models proposed, there
87 is still the need to further explore the epidemiology of *Xf* by integrating biological elements
88 influencing the *Xf* disease spread and growth mechanisms and patterns.

89 To contribute to the effort of developing integrated modelling approaches, in view also of the need
90 of supporting rational disease management, we propose a *Xf* Eco-epidemiological Model (XEM)
91 describing the continuous spread of *Xf* in an area. XEM is a spatially explicit mechanistic model
92 considering the following biological processes: i) the growth of the bacterium into the xylem of the
93 host plant, ii) the acquisition of the pathogen by the vector from an infected plant, and its
94 transmission to healthy plants, iii) the basic elements of the vector population dynamics, iv) the
95 dispersal of the vector. The environmental drivers affecting *Xf* epidemic dynamics are considered in
96 the model in terms of the impact on both the vector population dynamics and the development of
97 the bacterial population in the host plant. XEM describes the spatio-temporal dynamics of the
98 disease and the vector in a continuous or patchy landscape, with any composition of the plant
99 community.

100 Through the description of the landscape structure and the accurate calibration of the functions'
101 parameters, XEM can easily be adapted to describe any specific context and management strategies.
102 XEM is a suitable tool to evaluate the effectiveness of different risk reducing options and practices
103 aimed to the management of the disease pressure and spread, as well as to compare the efficacy of
104 strategies aimed at the eradication of new outbreaks.

105 In section 2.1 we describe the mathematical formulation and the biological assumptions of XEM. In
106 section 2.2 we apply the model to the Apulia outbreak of *Xf*, therefore the model components and
107 the parameterization for the case study are presented. The management strategies and scenario
108 analysis approach are explained in section 2.3. The results of the scenario analysis on infection
109 spread and management strategies are reported in Section 3. Discussion and conclusion are
110 presented in Section 4.

111

112 2. Materials & Methods

113 2.1. Mathematical formulation

114 XEM describes the spread dynamics of Xf in a spatial domain (Ω) during the time interval $[0, T]$.

115 XEM is based on the following biological assumptions:

- 116 • The univoltine biological cycle of the vector *P. spumarius* is here simplified considering two
117 phenological stages: the pre-imaginal stage and the adult stage. The two stages do not overlap.
118 In XEM, an adult vector can become infected solely by feeding on an infected plant. Once
119 infected, the vector can transmit the bacterium feeding on other plants, infecting and/or re-
120 infecting (i.e., increasing the bacteria load) them. The pre-imaginal stage is not able to acquire
121 neither to transmit the bacterium.
- 122 • Vector population dynamics are represented in a simplified way, the phenological processes and
123 events are described as occurring at pre-defined times in the year, depending on the site under
124 consideration. Change in population abundance is described only for the adult stage by means
125 of a site-specific natural mortality function. The initial conditions for the adult stage are set equal
126 to a site-specific maximum abundance interpreted as the local population carrying capacity. If
127 no external mortality factor is applied (e.g., pre-imaginal or adult control), each year adult
128 population dynamics has the same initial conditions, this assumption corresponds to the case in
129 which adult fecundity exactly compensates pre-imaginal mortality.
- 130 • Vectors move in the spatial domain. Only individuals in the adult stage can disperse and the
131 dispersal behaviour is modelled by means of a random walk motion. Vector long-distance
132 dispersal due to both human-assisted or natural movement is disregarded.
- 133 • The health status of a plant is described by the bacterial load titre in the xylem. In an infected
134 plant, the bacterial load titre grows due to the multiplication of the bacterial population within
135 the plant. A plant can receive multiple successful inoculums of the disease pathogen due to the
136 feeding of the infected vectors. These multiple inoculums also contribute to bacterial population
137 growth. We disregard plant mortality depending on bacterial load, therefore for a high level of
138 bacterial load titre the plant remains a source of bacteria for adult vectors. This simplified
139 assumption can be acceptable for a relatively short time period relevant for management
140 consideration, as considered in this paper.
- 141 • Successful transmission of the pathogen to the host plant is described by a transmission function
142 that considers: i) the vector feeding behaviour (also including the vector preference for the
143 target host), ii) the capacity of the vector to transmit the pathogen, iii) the susceptibility (s) of a

144 specific host plant (species or cv) to the pathogen. The possibility that vectors take and spread
145 the disease is influenced by the bacterial titre in the host plant.

146 • XEM considers only the short-range spread of the disease. We assume the disease to propagate
147 solely by the natural local dispersal and the feeding activities of the vectors. Long jumps of the
148 disease, due to natural or human-assisted dispersal of infected vectors, or to the trade of
149 infected plant material are not included in the model.

150 The model state variables are

151 • The abundance of infected adult vectors in the spatial point x at time t ($\gamma(x, t)$). The variable
152 $\gamma(x, t)$ assumes values in the range $[0, A(x, t)]$, where $A(x, t)$ is the adult vector abundance.
153 The abundance of uninfected adult vectors can be calculated as the difference between the
154 vector population abundance and the abundance of infected vectors ($A(x, t) - \gamma(x, t)$). $\gamma(x, t)$
155 is equal to 0 during the pre-imaginal stage.

156 • The health status of a host plant in the spatial point x at time t ($\varphi(x, t)$). The health status of a
157 host plant represents the level of bacteria load in that plant at time t , and it assumes values in
158 the range $[0,1]$ as it is normalized to a maximum level of bacteria load (see Tab. 3). In a non-
159 infected plant, the bacterium is absent, therefore $\varphi(x, t) = 0$. In an infected plant, $\varphi(x, t)$ is
160 greater than 0 and proportional to the bacteria load in the plant.

161 For the sake of clarity, hereinafter, $\varphi(x, t)$ and $\gamma(x, t)$ will be reported without their parameters.

162 The spread in space and time of the disease is described through a nonlinear system composed of a
163 parabolic partial differential equation for γ and a first-order ordinary differential equation for φ :

164

$$165 \quad \dot{\gamma}(x, t) = d\Delta\gamma(x, t) - M\gamma(x, t) + b(x, t)(A(x, t) - \gamma(x, t))\varphi(x, t) \quad [1]$$

$$166 \quad \dot{\varphi}(x, t) = [s l(x, t) \gamma(x, t) + F(t)\varphi(x, t)](1 - \varphi(x, t)) \quad [2]$$

$$167 \quad \partial_\nu \gamma(x, t) = \nabla \gamma(x, t) \cdot \nu(x) = 0$$

$$168 \quad \varphi(x, 0) = \varphi_0(x), \quad \gamma(x, 0) = \gamma_0(x)$$

169

170 where Δ is the Laplacian operator, ν is the normal versor on the boundary of Ω , ∂_ν stands for the
171 outward normal derivative on the boundary of Ω , $\varphi_0(x)$ and $\gamma_0(x)$ are the initial conditions, i.e.,
172 the status of the system at $t = 0$. The parameters of the XEM are defined in Table 1. The biological
173 meaning of the parameters and their estimation are reported in section 2.2.

174 The spatial domain Ω is approximated with a grid (mesh), considering the discrete counterpart of
 175 Neumann homogeneous boundary conditions on the discrete scheme (Brezis, 1986). The structure
 176 of the mesh is defined according to the characteristics of the landscape considered. In a continuous
 177 and homogeneous landscape, the host plants are placed in the nodes of the mesh and arranged in
 178 a continuous space with regular or irregular space among plants. In a patchy landscape, the host
 179 plants are present in restricted areas surrounded by unsuitable habitats or plants for the bacterium.
 180 This patchy spatial configuration can support metapopulation analysis of disease dynamics. Vectors
 181 are present in the whole Ω and the vector stage varies in time according to vector phenological
 182 dynamics.

183 Mathematical and numerical analysis of the model is detailed in Bazarra et al. (2022). Since we
 184 assume that functions $b(x, t)$ and $l(x, t)$ are positive, globally bounded and Lipschitz-continuous,
 185 the same existence, uniqueness and regularity properties still hold for the solution of system
 186 proposed in Bazarra et al. (2022).

187

188 Table 1 - Parameters of the XEM.

Parameter	Name	Units	Description
d	Spread parameter of the vector	Spatial unit ² time ⁻¹	Parameter of the Laplacian operator related to the dispersal capacity of the vector
M	Natural mortality of the infected vector	Time ⁻¹	Mortality rate in the survival function of the infected vector population
b	Acquisition rate function of the vector	Time ⁻¹	Acquisition rate of bacteria by the vectors feeding on infected plants
$A(x, t)$	Vector population abundance	Pure number	Population abundance of adult vectors (infected and non-infected) at time t in a spatial unit x
s	Plant susceptibility rate	Time ⁻¹	Probability in the time unit that a not-infected susceptible plant becomes systematically infected after the inoculation of bacteria by an infected adult vector during a day
$l(x, t)$	Bacterium inoculum	γ^{-1}	Bacteria load transmitted by a single vector in a successful feeding on a plant in a day

$F(t)$	Bacterial population growth function	Time ⁻¹	Time-dependent bacterial population growth rate in infected plants
--------	--------------------------------------	--------------------	--

189

190 2.2. Model application

191 XEM is applied to the current epidemics of *Xf* subsp. *pauca* in olive groves in the Apulia Region
 192 (Southern Italy). In 2013, *Xf* was identified in the Salento peninsula, near Lecce in the southern part
 193 of the Apulia, where it infected millions of olive trees and caused the death of many of them. At the
 194 beginning of 2019, the *Xf*-infected area included approximately 718,000 ha in the Apulia Region
 195 (REGULATION (EU) 2020/1201, 2020; Saponari, Giampetruzzi, et al., 2019). The spread of *Xf* is still
 196 ongoing, seriously threatening the Apulian olive sector.

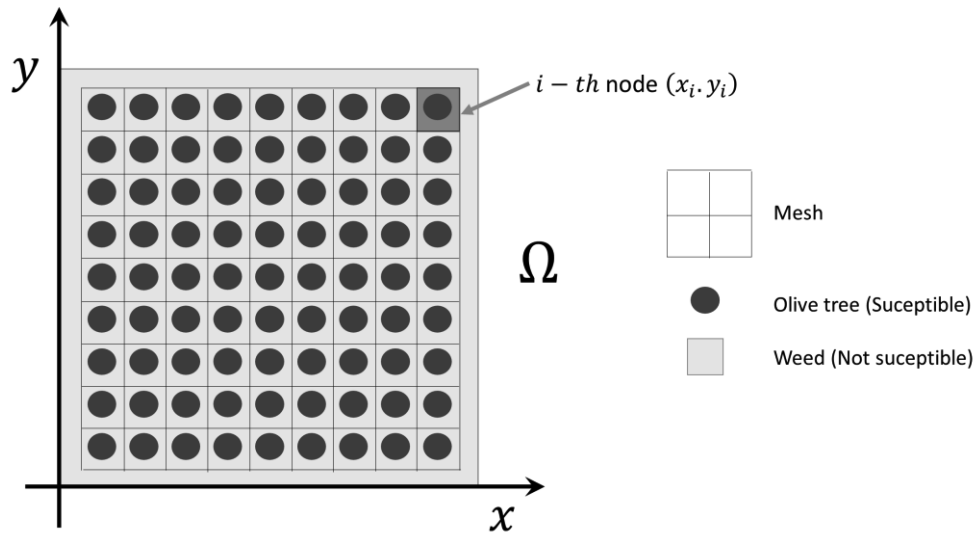
197 Results of scientific studies conducted in the context of the Apulian olive groves are used for
 198 estimating model functions and parameters related to the growth functions of the bacterium, the
 199 development of symptoms, the susceptibility of the different cultivars, and the phenology of the
 200 vectors. In the model application, the meadow spittlebug *P. spumarius* is considered the vector of
 201 *Xf*. To compensate for the lack of experimental data regarding the other functions and parameters
 202 of the model, we referred to data in the EFSA Update of the scientific opinion on the risks to plant
 203 health posed by *Xylella fastidiosa* in the EU territory (2019).

204

205 2.2.1. Landscape structure

206 Apulia is characterized by large olive groves with olive trees planted generally at large distances
 207 (e.g., 6- 10 meters) (Strona et al., 2017). We represented this landscape by defining a homogenous
 208 mesh of 10 km x 10 km with equally spaced host plants. The nodes of the mesh are the spatial units
 209 and represent cells of 10 x 10 m. At the centre of the node, there is a susceptible olive tree. We
 210 assumed the herbaceous cover between the hosts as not susceptible (Figure 1) so only olive-to-olive
 211 transmission is considered.

212 In this work, we explored different disease dynamics scenarios by applying XEM with different plant
 213 physiological responses and vector population abundance (Di Serio et al., 2019). Since the situation
 214 in the Apulian infected area is characterized by homogeneous fields cultivated with a predominant
 215 olive cultivar, within a simulated scenario the host plants' susceptibility is set equal for all nodes.
 216 The typical agroecological conditions in the Apulian olive growing region are included in the model.
 217 The time step of the simulations is set to 1 day and the time horizon to 5 years.



219

220 Figure 1 - Structure of the generic homogeneous landscape Ω configured to simulate the disease
 221 dynamics in the conditions of Apulian large olive groves. Host plants (green circle) are equally spaced
 222 defining a regular grid (black matrix). A non-susceptible weed covers the space between hosts.

223

224 2.2.2. Vector phenology and survival

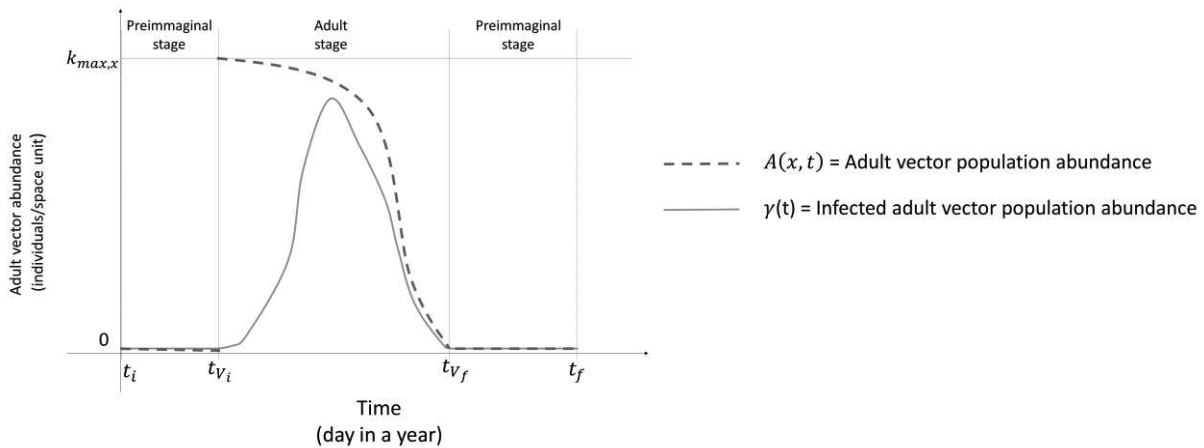
225 The pre-imaginal stage occurs from the beginning of the year (t_i) up to the appearance of the adult
 226 stage (t_{V_i}) and after oviposition (t_{V_f}) until the end of the year (t_f) (Figure 2). The adults emerge
 227 from pre-imaginal stage and occurs in the time interval $[t_{V_i}, t_{V_f}]$. In the this time interval, the adults

228 population abundance varies according to the survival profile $A(x, t) = k_{max,y} * \sqrt{\frac{t_{V_f}-t}{t_{V_f}-t_{V_i}}}$, starting

229 from the site-specific maximum carrying capacity ($k_{max,x}$) at t_{V_i} . In the time interval $[t_{V_i}, t_{V_f}]$, the
 230 abundance of infected adults is defined by $\gamma(x, t)$.

231 Based on the climatic conditions of Apulia and the data on adults emergence available in the
 232 literature (Bodino et al., 2020; Di Serio et al., 2019), we set $t_{V_i} = 130$ (May 10th) and the end of
 233 period of vector feeding activities at $t_{V_f} = 300$ (October 27th).

234 The natural mortality rate of the infected adults (the parameter M in Eq. 1) has been estimated
 235 equal to 0.015 day^{-1} . This value describes a survival curve that well approximates available data on
 236 the duration of the adult stage and the population abundance of *P. spumarius* (Bodino et al., 2019;
 237 Bodino, Demichelis, et al., 2021; Di Serio et al., 2019).



239

240 Figure 2 - Exemplification of the dynamics of infected vector abundance in 1 year of simulation
 241 where $t_i = 1$ is the first day of the year, t_{V_i} is the day of adult emergence, t_{V_f} is the day when the
 242 last adult disappears, and $t_f = 365$ is the last day of the year.

243

244 2.2.3. Vector dispersal

245 Only vectors in the adult stage can disperse. Their dispersal behaviour is modelled by means of a
 246 random walk motion through the Laplace operator Δ and its diffusive coefficient d in Eq. 1. For the
 247 vector dispersal capacity, we referred to the median dispersal distance of *P. spumarius*, estimated
 248 by EFSA equal to 800 m/year (EFSA PLH Panel, 2019). The value of the diffusive coefficient d is
 249 derived using a simulation procedure. An initial population of 1000 adult vectors is released in the
 250 centre of the landscape at time t_{V_i} . We selected the value of d such that at t_{V_f} half of the vector
 251 population is in a circular area of 800 meters of radius from the point of release. The estimated
 252 value of the parameter is $d = 1500\text{m}^2\text{day}^{-1}$.

253

254 2.2.4. Bacteria acquisition rate

255 To estimate the vector bacteria acquisition rate $b(x, t)$ (Eq. 1) we referred to the median value
 256 (12.08%) of the elicited distribution of acquisition rates of the vector reported in the EFSA Opinion
 257 (EFSA PLH Panel, 2019), representing the daily probability of acquisition of the bacteria in optimal
 258 conditions (e.g., the vector feeds on highly infected plants only). In XEM, the acquisition rate of the
 259 vector in the EFSA Opinion is used to estimate the maximum value for $b(x, t)$ (b_{max}), achievable
 260 when $\varphi = 1$. To estimate b_{max} , a population of 1000 non-infected vectors feeding on highly

261 infected host plants is simulated. After one day of feeding activity, we obtained 12.08% of the
262 vectors infected with $b_{max} = 0.0995 \text{ day}^{-1}$.

263 In XEM, b_{max} is scaled according to the health status of the plant. We assumed that the probability
264 of a successful daily feeding activity depends both on the bacterial titre in the plant and on the time
265 spent in the feeding activity by the vector in a day. To represent this process, we used the Ivlev
266 model (Ivlev, 1961), a non-linear functional response widely used to describe the predator's
267 efficiency in searching and capturing the prey as a function of prey density: $p(x) = q * (1 - e^{-j p})$.
268 In XEM, we set $p = \varphi$, $q = b_{max}$, and $j = 50$. We select the value of j such that the bacteria
269 acquisition rate is close to b_{max} when $\varphi(x, t) = 0.1$, corresponding to a symptom's severity in the
270 host plant equal to three (see Table 3).

271

272 2.2.5. Bacterial population growth function

273 The bacterial population in an infected plant increases following the function $F(t)$ (Eq. 2). Bacterial
274 population growth varies according to the physiological state of the plant, the environmental
275 conditions, and plant susceptibility.

276 Concerning plant physiology and environmental conditions, three periods in a year are identified: i),
277 the physiological state of the host plant is not favourable to bacterial growth, so $F(t) = 0$, ii) the
278 host is in a favourable physiological state for the bacteria, but the growth is sub-optimal due to not
279 favourable environmental conditions (e.g., high temperature and low relative humidity), so the
280 bacterial population grows at a low rate, $F(t) = r_L$, iii) both the host physiological state and the
281 environmental conditions are favourable, the bacterial population grows at a high rate, $F(t) = r_H$.
282 The bacterial population growth function is defined as follows:

283

$$284 \quad F(t) = \begin{cases} 0 & t \in [1, t_{H_1}) \cup [t_{H_4}, 365] \\ r_H & t \in [t_{H_1}, t_{H_2}) \cup [t_{H_3}, t_{H_4}) \\ r_L & t \in [t_{H_2}, t_{H_3}) \end{cases} \quad \text{with } 1 < t_{H_1} < t_{H_2} < t_{H_3} < t_{H_4} < 365.$$

285

286 For the Apulian case, we set $t_{H_1} = 129$ (May 8th), $t_{H_2} = 212$ (July 29th), $t_{H_3} = 242$ (August 29th),
287 $t_{H_4} = 287$ (October 12th). Growth rates depend also on the host plant susceptibility (Giampetruzzi
288 et al., 2016; Saponari, Loconsole, et al., 2019). We used data from a field study on the dynamics of
289 Xf spread and symptoms development, conducted in Apulia in 2016 and 2017 (Montes-Borrego, M.

290 et al., 2017), to derive the growth rates for different periods in the year and hosts susceptibility. We
 291 considered a susceptible olive tree cultivar (Ogliarola) and a tolerant cultivar (Leccino). The best
 292 estimates for the bacteria growth functions (Table 2) are obtained starting from an initial bacteria
 293 inoculum $\varphi_i = 0.0001$. In the Apulian datasets, a percentage of host-plants tolerant to infection
 294 (N_s) throughout all the observation period is reported. This cultivar-dependent percentage (Table
 295 2) has been considered in the model.

296

297 Table 2 – Estimates of the percentage of not susceptible plants, and of the high and the low bacterial
 298 population growth rates for the susceptible host plants (cv Ogliarola) and the tolerant host plants
 299 (cv Leccino).

	Percentage of not susceptible plants N_s	High growth rate r_H	Low growth rate r_L
Susceptible host plants (cv Ogliarola)	7 %	0.020	0.010
Tolerant host plants (cv Leccino)	0.287	0.017	0.009

300

301 2.2.6. Plant susceptibility

302 According to EFSA (2019), plant susceptibility is defined as the probability that a non-infected
 303 susceptible plant becomes systematically infected as a consequence of the feeding activity of an
 304 infected adult vector during a day. We set the plant susceptibility (s) for tolerant host plant equal
 305 to the first quartile of the distribution for susceptibility elicited by EFSA (2019) ($s = 0.09$), and to
 306 the median value of that distribution for susceptible host plants ($s = 0.14$).

307

308 2.2.7. Bacteria transmission to the plant

309 Infected vectors inoculate the bacteria into the host by feeding on the xylem-sap of the plant. In a
 310 plant not yet infected, bacteria inoculum triggers the process of plant infection. The bacteria
 311 inoculum per vector in a day is estimated equal to $l = 1 * 10^{-4}$, based on field studies on the
 312 dynamics of symptoms development X_f (Montes-Borrego, M. et al., 2017).

313 In XEM, the transmission of the bacteria from the vector population to the host plant population
 314 takes into account a density-dependent reduction ($l(\cdot) = l * e^{-4\gamma}$) with the increase of vector
 315 population, estimated based on results obtained by Montes-Borrego, M. et al (2017). This is to
 316 account for both the increase of the probability of vector feeding in already infected leaves of the

317 host plants and the effects of intra-species competition, leading to the selection of host plants other
318 than olive trees.

319

320 2.2.8. Symptoms severity

321 We assume that during the asymptomatic period the plant is infected and infectious, but it does not
322 manifest any visual symptoms. To correlate the level of infection of the plant $\varphi(t)$ with the severity
323 of the symptoms, we referred to Saponari et al. (2019). These authors tested bacterial population
324 load (C) for Ogliarola and Leccino cultivars and reported the estimation of symptoms severity,
325 measured on a 6-points scale (0 - no symptoms; 5 -maximum level of symptoms, i.e., the plant is no
326 longer productive). In Table 3, we report the thresholds of bacteria load and the corresponding
327 values of plant health status for each class of symptoms severity.

328

329 Table 3 - Intervals of bacteria load ($\text{Log}C$) and plant health status ($\varphi(t)$) for the six symptoms severity
330 classes.

Bacteria load	Plant health status	Plant symptoms
<i>LogC</i>	$\varphi(t)$	severity
0	0	0
0 – 5.06	0 – 0.0115	1
5.06 – 5.55	0.0115 – 0.0352	2
5.55 – 6.03	0.0352 – 0.107	3
6.03 – 6.52	0.107 – 0.328	4
6.03 – 7.00	0.328 – 1	5

331

332 2.3. Simulation of epidemiological scenarios

333 The XEM, parameterized as in Section 2.2., is applied to explore the spatio-temporal dynamics of Xf
334 considering two levels of vector abundance (high and low) and two levels of host plant susceptibility
335 (high and low) (Table 4). Based on data published in Di Serio et al. (2019), we defined 20 adults per
336 m^2 as the high level of vector population and 1 adult per m^2 as the low level of the vector population.

337 Table 4 – Parameter used in the definition of the four simulation scenarios on epidemiological
338 dynamics of Xf in Apulia olive groves.

Epidemiological Simulation Scenario (Epidem)		Density of vector population	
		High (20 adults/m ²)	Low (1 adult/m ²)
Susceptibility of the host plant	High $s = 0.14, r_H = 0.02; r_L = 0.01$	Epidem-HH	Epidem-HL
	Low $s = 0.09, r_H = 0.017, r_L = 0.009$	Epidem-LH	Epidem-LL

339

340 The onset of infection is simulated through the successful inoculation of nine susceptible plants in
341 an area of 30 m radius in the centre of a free area (inoculation point). Disease dynamics are analysed
342 for 5 years, with a temporal resolution of 1 day.

343 The spatio-temporal dynamics of the disease in the four scenarios are assessed at the end of each
344 simulation year according to the following output variables:

- 345 • Infected host plants: Number of infected host plants;
- 346 • Disease pressure: Mean value of health status of the host plants (φ). The mean is computed only
347 on infected plants, i.e., $\varphi > 0$;
- 348 • Infected vector pressure: Mean annual density of the population abundance of infected vectors.
349 The mean is calculated only during the period of adult presence;
- 350 • Disease spread: Maximum distance of the infected plants from the inoculation point.

351 The simulations were conducted in Matlab (version R2018b), applying the finite element approach
352 to discretization (further details are reported in Bazarra et al., 2022).

353

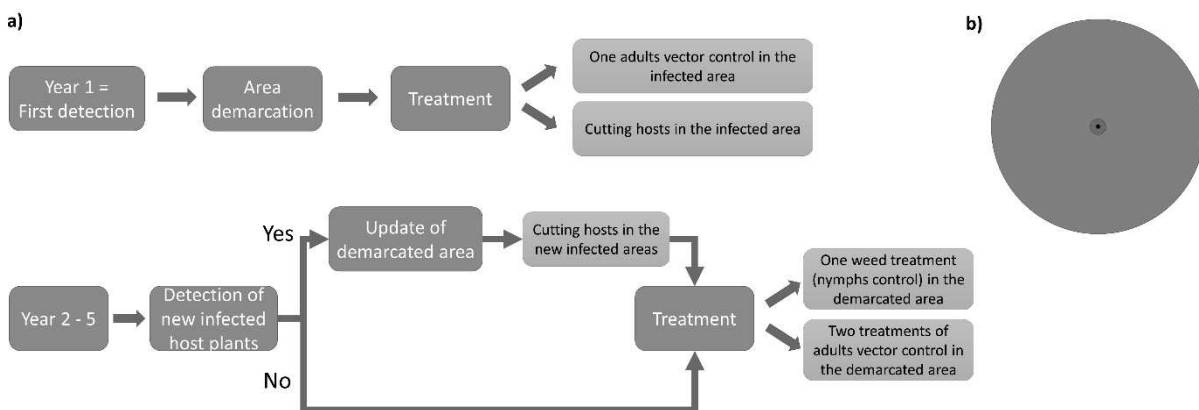
354 2.4. Simulation of management scenarios

355 The definition of the management strategies to be tested is based on the European Legislation in
356 force at the time the study was carried out (Council Directive 2000/29/EC, 2000; Decision (EU)
357 2015/789, 2015; Decision (EU) 2017/2352, 2017), focusing on eradication measures.

358 In our study, the management strategies are applied from the first detection of an infected plant in
359 a free area (i.e., an area where infected plants are not reported) till the end of the simulation period.
360 Following the detection of an infected plant, three areas are marked out around the detection point
361 (area demarcation process). The first area, with a radius equal to the value of the cutting radius, is

362 defined as the infected area. The second area is a circular crown with a minimum radius equal to
 363 the cutting radius and a major radius of 5000m and is defined as the buffer zone. The infected area
 364 and the buffer zone constitute the demarcated area. Immediately after the detection, all potential
 365 *Xf* host plants are cut and one adult vector control treatment is performed in the infected area. In
 366 the years following the detection till the end of the simulation period, the management strategy
 367 applied in the demarcated area consists of one weed treatment, carried out in spring to control the
 368 nymph population, and two vector control treatments, carried out in late spring and in the summer.
 369 The vector control treatments have the aim of reducing both the adult vector population in the
 370 current year and the vector population in the next year, as a result of a reduction in the number of
 371 adults and then in the number of overwintering eggs that are laid. Therefore, the repetition of
 372 treatment over years leads to a significant reduction in the abundance of the vector. Figure 3
 373 graphically represents the management scheme applied in the scenario analysis. The sequence and
 374 type of control treatments to be performed are different in the first year of detection than in
 375 subsequent years because it is not possible to carry out weed treatment for nymphs control in the
 376 first year of detection. Management strategies are applied for 5 years.

377



378

379 Figure 3 - Overall structure of the management strategy tested in the simulation scenario analysis.
 380 On the left (a) is presented the sequence and type of management actions to be implemented
 381 according to the simulation year: year 1 is the year in which the first infected plant is detected, from
 382 year 2 to year 5 are the following years until the end of the simulation period. On the right (b) is
 383 reported the spatial structure of the demarcated area is displayed. The central black dot is the plant
 384 detected as infected, the red area is the infected area, and the blue area is the buffer zone.

385

386 Based on the overall structure of the management strategies described in Figure 3, four factors
387 relevant to eco-epidemiological dynamics and of interest to international policymakers are tested:
388 efficacy of adult vector and weed control actions, the radius of the cutting area, time of the first
389 detection, time to intervention. For each factor two levels are tested, defining a total of 16
390 management scenarios. Low efficacy of control treatments corresponds to 60% of nymph mortality
391 following weeds treatments and 50% of adult mortality following chemical control of the adults,
392 while high efficacy corresponds to 80% of nymph mortality following weeds treatments and 90% of
393 adult mortality following chemical control of the adults. The large cutting radius corresponds to 100
394 m, the small cutting radius is set to 50 m. Two times for the first detection were considered: early
395 and late detection occurs 3 and 4 years after inoculation, respectively. Finally, we tested the impact
396 of two different implementation times of the control actions. Early and late intervention occur 30
397 and 60 days after the detection, respectively. The early intervention corresponds to the first period
398 of adult flight (just after adults' emergence).

399 The efficacy of the management strategies scenarios was assessed by considering the characteristics
400 of the worst-case scenario, i.e., the eco-epidemiological scenario where at the 5th year after
401 infection the infected area was greater. The management strategies were applied for 5 years,
402 including the years of the first detection. At the end of the simulation, the X_f infection dynamics
403 were assessed. We checked whether the infection was completely eradicated or not and the spread
404 of the infection, measured in terms of the proportion of infected area under managed conditions
405 compared with the area obtained in the unmanaged epidemiological scenario at the same time
406 horizon.

407

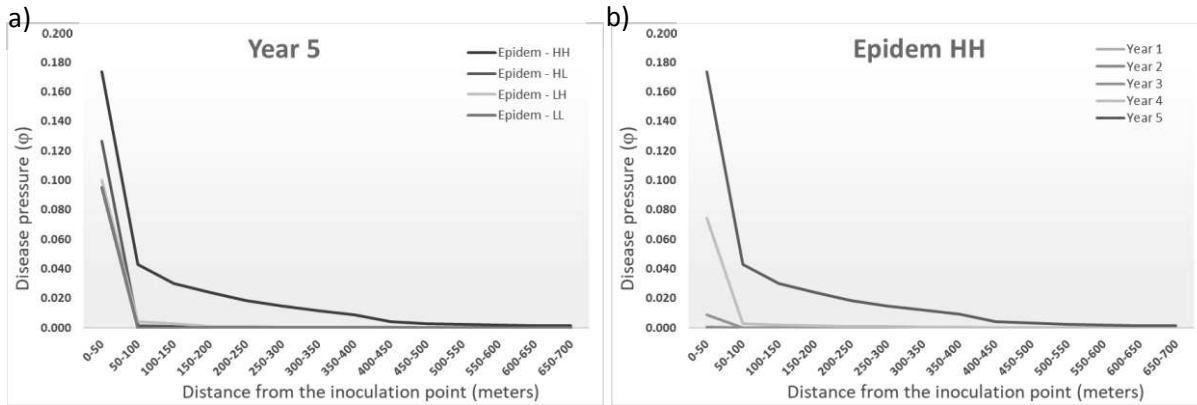
408 3. Results

409 3.1. Disease pressure

410 The spatio-temporal dynamics of the infection in the simulation scenarios are represented in Figure
411 4. The mean disease level in the infected plants decreases with a common pattern over the spatial
412 dimension in the four scenarios (Figure 4-a). However, only in the Epidem - HH, the mean level of
413 the disease is at least equal to the first level of severity of symptoms outside the area of radius 50-
414 meter from the points of inoculum. In the Epidem - LH and Epidem - LL cases, the mean disease
415 levels never reach the third level of severity of symptoms. The temporal dynamics are then assessed
416 on the worst-case scenario, i.e., the one with the highest average disease pressure. In the Epidem -
417 HH scenario, the mean level of disease in infected plants grows very slowly in the first 3 years of

418 simulation (Figure 4-b). The threshold of visual detection of symptoms (i.e., severity class of 1) is
 419 exceeded in the fourth year of simulation up to 50 m from the inoculation site, in the fifth year
 420 symptoms are visible up to 300 m from the inoculation site.

421



422

423 Figure 4 - Distribution of the disease pressure (mean value of the health status of the infected plants)
 424 according to the distance from the points of inoculum. a) Scenario comparison: results obtained at
 425 the end of the simulation period for the four simulation scenarios. b) Temporal dynamics: results
 426 obtained at the end of each of the five simulation years in the scenario HH.

427 Epidem - HH: High plant susceptibility-High vector abundance; Epidem - HL: High plant susceptibility-Low
 428 vector abundance; Epidem - LH: Low plant susceptibility-High vector abundance; Epidem - LL: Low plant
 429 susceptibility-Low vector abundance.

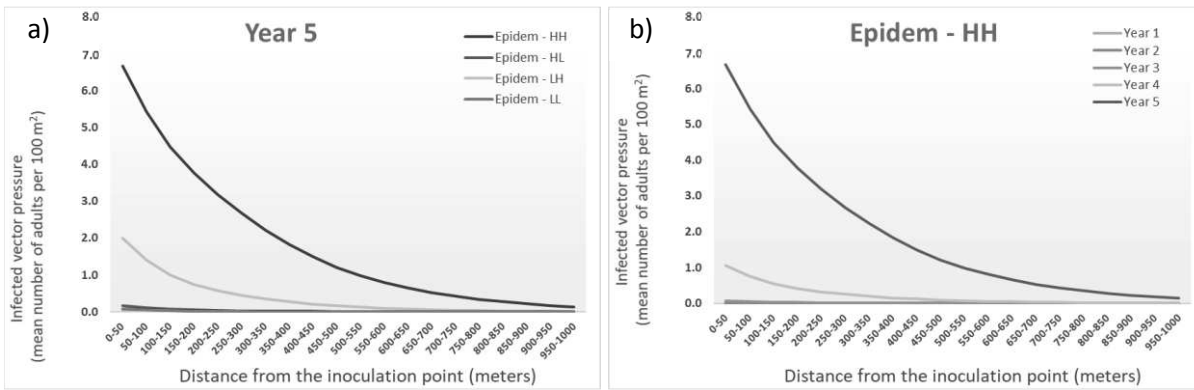
430

431 3.2. Infected vector pressure

432 The mean densities of infected vectors decrease with a common pattern over the spatial dimension
 433 in all the simulation scenarios, although the maximum population values are quite different (Figure
 434 5-b). The temporal dynamics of the density of infected vectors are shown for the scenario Epidem -
 435 HH in Figure 5-a.

436 In the last year of simulation, the highest mean density of infected vectors for the two scenarios
 437 characterized by a low vector abundance is equal to 0.16 (Epidem - HL) and 0.08 (Epidem - LL)
 438 vectors per 100 m². For the HH scenario, the mean density of infected vectors per 100 m² in the last
 439 year of simulation is greater than 1 only within the first 500 m from the inoculation point.

440



441

442 Figure 5 - Distribution of infected vector pressure (mean annual density per 100 m² of the population
 443 abundance of infected vectors) according to the distance (meters) from the points of inoculum. a)
 444 Scenarios comparison: Results obtained in the last year of simulation for the four simulation
 445 scenarios. B) Temporal dynamics: Results obtained for the 5 years of simulation in the scenario
 446 Epidem - HH.

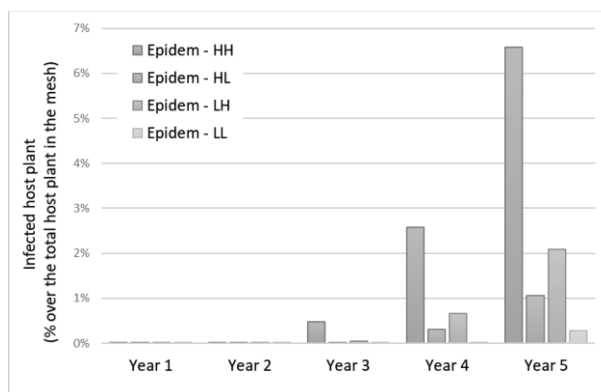
447 Epidem - HH: High plant susceptibility-High vector abundance; Epidem - HL: High plant susceptibility-Low
 448 vector abundance; Epidem - LH: Low plant susceptibility-High vector abundance; Epidem - LL: Low plant
 449 susceptibility-Low vector abundance.

450

451 3.3. Infected host plants

452 The annual distributions of infected host plants for each simulation scenario are shown in Figure 6.
 453 The highest number of infected plants (almost 70000, equal to 6.58% of the host plants in the
 454 landscape) occurred in the scenario Epidem - HH. In the Epidem - LL, there are less than 3000
 455 infected plants at the end of the 5th year of simulation.

456



457

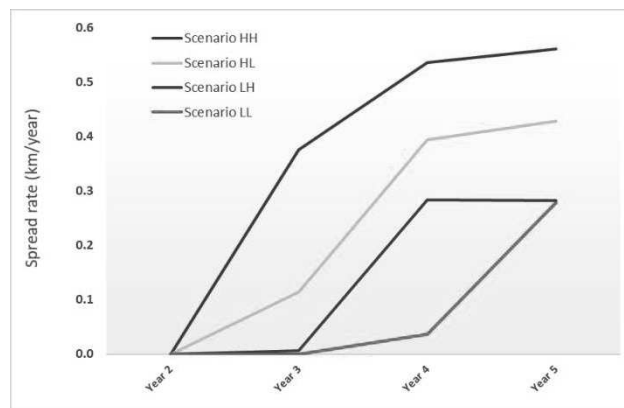
458 Figure 6 - Distribution of the infected host plants at the end of each simulation year in the four
 459 simulation scenarios.

460

461 3.4. Disease spread

462 The spread of the infection has been assessed based on the dynamics of the 5 years of simulation,
463 focusing on the initial build-up of an invasion front. At the end of the simulation period, the
464 maximum distance of infected plants from the initial inoculation point is approximately 1500 m for
465 scenario HH, 970 m for LH, 600 m for HL and 340 m for LL. The spread rates for each scenario,
466 expressed as km travelled by the invasion front per year, are reported in Figure 7. The spread rates
467 increase over time, with different non-linear patterns based on the simulation scenario considered.
468 At the end of the simulation period, the spread rate is 0.56 km per year for the scenario HH, 0.43
469 km per year for LH and about 0.28 km per year for HL and LL.

470



471

472 Figure 7 - The spread rate of the disease (km/year) in the four simulation scenarios.

473

474 3.5. Management option efficacy

475 The basic epidemiological scenario used to define the management strategies was scenario Epidem-
476 HH, high density of vector population and high susceptibility of the host plant to Xf.

477 The results of the scenario analysis on management strategies are shown in Table 5. In nine of the
478 16 management scenarios, Xf infection was successfully eradicated, with different impacts in terms
479 of the spread of infection depending on the strategy adopted. From the outcomes, the effects of
480 control efficacy, cut radius, time to detection and intervention can be derived.

481 The greatest effect on eradication is determined by the efficacy of nymphs and adult control
482 treatments. In the eight scenarios where high efficacy of control actions was simulated, the infection
483 was eradicated at the end of the assessment period. In the eight scenarios where control actions
484 have low efficacy, only one management strategy leads to eradication: early detection, early
485 intervention, and a cut radius of 100 m. In all the other management scenarios with low vector

486 control efficacy, eradication is not achieved. Furthermore, in the seven scenarios where eradication
 487 is not achieved, the management actions reduce the pressure of the infected vectors to less than
 488 0.035 vectors/m².

489

490 Table 5 - Results of the simulation scenarios on management strategies for the infection of *Xylella*
 491 *fastidiosa*.

492

Factors and levels					Simulation scenario 5 years after detection	
Management Scenario	Control efficacy	Detection	Time to intervention	Cut radius	Successfully eradication	Percentage of infected area*
Manag-01	High	Early	Early	Large	Yes	13.0%
Manag-02				Small		10.8%
Manag-03			Late	Large		13.2%
Manag-04				Small		11.9%
Manag-05		Late	Early	Large		18.2%
Manag-06				Small		15.4%
Manag-07			Late	Large		18.3%
Manag-08				Small		18.0%
Manag-09	Low	Early	Early	Large		13.4%
Manag-10	Low	Early	Early	Small	No	14.7%
Manag-11				Late		Large
Manag-12			Small			17.9%
Manag-13			Late	Early		Large
Manag-14		Small				22.1%
Manag-15		Late		Large		27.0%
Manag-16				Small		23.0%

493

494 * Percentage of infected area compared to the area of infection detected at the same time horizon in the
 495 unmanaged epidemiological scenario (Epidem-HH): the 8th and 9th year of epidemiological simulation for
 496 early and late detection, respectively

497

498 4. Discussion and conclusion

499 In XEM, the main biological processes related to the disease dynamics are described in detail, with
500 reference to i) the vector acquisition of the bacterium from the plant, ii) the bacterial transmission
501 rate from the vector to the plant, iii) the growth process of the pathogen inside the plant, and iv)
502 the vector's dispersal. Rates and functions describing these processes can be adapted to
503 environmental characteristics and host susceptibility. Process functions and parameters can also be
504 adapted to different vector species and *Xf* subspecies or strains.

505 The application of XEM to the case of the spread of *Xf* in Apulia allowed estimating the spread rate
506 of the infection under the hypothesis that the bacterium is spread by natural vector dispersal only.
507 The disease spread rate increases year by year and reaches about 0.6 km per year 5 years after the
508 initial inoculation. The average annual spread of the infection is expected to be considerably greater
509 if long jumps are considered (Bodino, Cavalieri, et al., 2021).

510 A critical issue in dealing with emerging diseases is related to knowledge gaps (Tamborindéguy et
511 al., 2017). The lack of historical data on biological processes makes it difficult to calibrate the models
512 on the analysed system, even when it is possible to describe the dynamics in formal and modelling
513 terms. The estimations of XEM parameters are affected by a set of variability and uncertainty
514 sources related to model assumptions and to the eco-epidemiological system that is studied.

515 The susceptibility of plants influences the growth rate of the bacterial population in the plant, and
516 it has a significant impact on the duration of the asymptomatic period. The XEM allows for the
517 evaluation of the progression of the disease in the plants. The possibility of defining specific growth
518 rates for different periods of the year (to account for plant phenology and environmental
519 conditions) and host plant susceptibilities (among species or individuals within the same species),
520 allows for the application of XEM to several agroecosystems. Furthermore, associating the host
521 plant health status with a scale of symptoms onset allows for modelling any type of disease latency
522 (i.e., the period in which the pathogen is present in the plant, but it is not detectable, neither visually
523 nor with laboratory diagnostic procedures). The calibration of XEM parameters related to disease
524 growth and latency period requires knowledge on the susceptibility of the host plants/cultivars of
525 interest and the specific bacterial growth mechanisms within these species. Recent studies are
526 bringing evidence regarding the importance of weeds in the *Xf*-olive tree-vector pathosystem, as
527 they represent both the habitat where the vector nymphs complete their development and a
528 possible reservoir for the bacterium (Anița et al., 2021; Brunetti et al., 2020). In our study, the
529 herbaceous plant community has been considered only as support in the pre-imaginal stage

530 development. Further developments of the model may include the weeds as a potential host for the
531 bacterium in order to assess their contribution to the epidemiology of *Xf*-olive tree-vector
532 pathosystem.

533 The variability related to vector spread rate and dispersal patterns can be addressed by modifying
534 the uncertainty distribution for the vector dispersal kernel. A different spread rate or a non-
535 homogenous distribution of the disease could have direct effects on the assessment of spatio-
536 temporal dynamics of disease spread and, therefore, on the assessment of management or
537 eradication strategies.

538 The vector acquisition rate can be modified to consider the within- and between-species variability
539 in the feeding rate and preference.

540 The density of the vector population is highly variable. Since the scenario results showed that it had
541 a strong impact on *Xf* spread, actions aimed to strongly reduce vector population abundance could
542 be key elements for the success of eradication strategies. For these reasons, careful studies to
543 estimate the abundance of the population should be preliminary to the implementation of the XEM
544 model.

545 In scenario analysis of epidemiological dynamics, the rate of successful transmission of the pathogen
546 from the infected vector to the host plant and from an infected plant to the vector are among the
547 parameters that most influence system dynamics. The results of new experimental studies on these
548 factors could easily be included in XEM.

549 The generality and flexibility of XEM make the model a suitable tool to better understand the disease
550 mechanisms and patterns and to evaluate the effectiveness of different risk reducing options and
551 practices devoted to the management of the disease pressure and spread. XEM can also be used for
552 the evaluation of management and/or eradication strategies. In our scenario analysis, the high
553 efficacy of vector and weed control intervention are identified as the key factors for a successful
554 eradication (in accordance with Anița et al. (2021)). The prompt intervention after infection
555 detection could limit the impact of *XF* when eradication is not achieved. From simulation outcomes,
556 it emerges that the management measures are effective if performed just after adults' emergence
557 (early intervention) limiting the density of infected vectors that rapidly increases over the favourable
558 season. This result is an example of useful information to support decision-making as it underlines
559 the importance of limiting the delay in applying control actions, other things being equal, in the
560 system considered.

561 The cut-off radius is crucial for eradication only when there is early detection and timely
562 intervention, and the efficacy of vector control is low. In these scenarios, the 100 m cut radius allows
563 achieving the eradication, whereas a smaller radius (50 m) does not allow this.

564 The management strategies influence the infection spread, measured in the percentage of the
565 infected area compared to the infected area in the unmanaged scenario. In particular, lower
566 infected areas occur in all the scenarios with early detection. In the scenarios where eradication is
567 not achieved, the spread of infection can be reduced by reducing the time of application of
568 intervention measures (early intervention).

569 From the analyses carried out, it emerges that further knowledge is needed on the main sources of
570 uncertainty in the eco-epidemiological system analysed, in particular the susceptibility of the host
571 plants, the rate at which the bacteria are acquired by the vector, the range of movement of the
572 vector and the delay in detecting the disease.

573 XEM could be used to assess the outcome of the application of different detection and control
574 strategies. Each process described in XEM (e.g., vector-plant transmission, asymptomatic period,
575 growth of the bacterium into the plant, vector phenology) is defined by specific parameters. The
576 inclusion in the model of detection/control strategies is simplified and requires only the estimation
577 of the impact that these actions have on related parameters of the model (e.g., a control action of
578 the vector will reduce the carrier's carrying capacity). Being spatially explicit, XEM allows assessing
579 the impact of actions only in the areas where they are implemented. Furthermore, the temporal
580 resolution of the model and the inclusion of the phenology of both host plants and vectors allows
581 the evaluation of the variability of the efficacy of the detection/control strategies according to the
582 period in which they are carried out.

583 The huge efforts and investments in research on *Xf* led to an increasing amount of knowledge on
584 both the bacterium (e.g., the basic mechanisms of disease infection and growth in the host plant)
585 and the vectors (e.g., phenology). However, this knowledge body of growing complexity urgently
586 needs integration into efficient and readily available tools to support strategies for preventing and
587 mitigating the effects of *Xf*. These tools should be able to stock up on low-scale (e.g., i-state model)
588 to high-scale (p-state model) knowledge (Caswell & John, 1992; Gyllenberg, 2007). XEM allows
589 integrating the scientific evidence at various spatial and temporal resolutions (from individual plants
590 to large-scale heterogeneous landscapes), including the effects of environmental drivers (climate
591 and land use) and climate change. Therefore, XEM could be implemented in control strategies for
592 *Xf* management at different levels, from field to regional, from operational to policy, supporting the

593 implementation of risk reduction options in plant health and for selecting control techniques and
594 guiding the development of IPM strategies at the farm- and area-wide-level.

595

596 References

597 Almeida, R. P. P., Wistrom, C., Hill, B. L., Hashim, J., & Purcell, A. H. (2005). Vector Transmission of
598 *Xylella fastidiosa* to Dormant Grape. *Plant Disease*, *89*(4), 419–424.

599 <https://doi.org/10.1094/PD-89-0419>

600 Anița, S., Capasso, V., & Scacchi, S. (2021). Controlling the Spatial Spread of a Xylella Epidemic.

601 *Bulletin of Mathematical Biology*, *83*(4), 32. <https://doi.org/10.1007/s11538-021-00861-z>

602 Bazarra, N., Colturato, M., Fernández, J. R., Naso, M. G., Simonetto, A., & Gilioli, G. (2022). Analysis
603 of a Mathematical Model Arising in Plant Disease Epidemiology. *Applied Mathematics &*
604 *Optimization*, *85*(2), 19. <https://doi.org/10.1007/s00245-022-09858-z>

605 Bodino, N., Cavalieri, V., Dongiovanni, C., Plazio, E., Saladini, M. A., Volani, S., Simonetto, A.,

606 Fumarola, G., Carolo, M. D., Porcelli, F., Gilioli, G., & Bosco, D. (2019). Phenology, seasonal
607 abundance and stage-structure of spittlebug (Hemiptera: Aphrophoridae) populations in
608 olive groves in Italy. *Scientific Reports*, *9*(1), 17725. [https://doi.org/10.1038/s41598-019-](https://doi.org/10.1038/s41598-019-54279-8)
609 [54279-8](https://doi.org/10.1038/s41598-019-54279-8)

610 Bodino, N., Cavalieri, V., Dongiovanni, C., Saladini, M. A., Simonetto, A., Volani, S., Plazio, E.,

611 Altamura, G., Tauro, D., Gilioli, G., & Bosco, D. (2020). Spittlebugs of Mediterranean Olive
612 Groves: Host-Plant Exploitation throughout the Year. *Insects*, *11*(2), 130.

613 <https://doi.org/10.3390/insects11020130>

614 Bodino, N., Cavalieri, V., Dongiovanni, C., Simonetto, A., Saladini, M. A., Plazio, E., Gilioli, G.,

615 Molinatto, G., Saponari, M., & Bosco, D. (2021). Dispersal of *Philaenus spumarius*

616 (Hemiptera: Aphrophoridae), a Vector of *Xylella fastidiosa*, in Olive Grove and Meadow

617 Agroecosystems. *Environmental Entomology*, 50(2), 267–279.

618 <https://doi.org/10.1093/ee/nvaa140>

619 Bodino, N., Demichelis, S., Simonetto, A., Volani, S., Saladini, M. A., Gilioli, G., & Bosco, D. (2021).
620 Phenology, Seasonal Abundance, and Host-Plant Association of Spittlebugs (Hemiptera:
621 Aphrophoridae) in Vineyards of Northwestern Italy. *Insects*, 12(11), Art. 11.
622 <https://doi.org/10.3390/insects12111012>

623 Brezis, H. (1986). *Analisi funzionale: Teoria e applicazioni* (Vol. 9). Liguori Editore Srl.

624 Brunetti, M., Capasso, V., Montagna, M., & Venturino, E. (2020). A mathematical model for *Xylella*
625 *fastidiosa* epidemics in the Mediterranean regions. Promoting good agronomic practices
626 for their effective control. *Ecological Modelling*, 432, 109204.
627 <https://doi.org/10.1016/j.ecolmodel.2020.109204>

628 Caswell, H., & John, A. M. (1992). From the Individual to the Population in Demographic Models. In
629 *Individual-Based Models and Approaches in Ecology*. Chapman and Hall/CRC.

630 Cavalieri, V., Altamura, G., Fumarola, G., di Carolo, M., Saponari, M., Cornara, D., Bosco, D., &
631 Dongiovanni, C. (2019). Transmission of *Xylella fastidiosa* Subspecies *Pauca* Sequence Type
632 53 by Different Insect Species. *Insects*, 10(10), E324.
633 <https://doi.org/10.3390/insects10100324>

634 Cavalieri, V., & Porcelli, F. (2017). Main insect vectors of *Xylella fastidiosa* in Italy and worldwide. In
635 *Xylella fastidiosa & the Olive Quick Decline Syndrome (OQDS). A serious worldwide*
636 *challenge for the safeguard of olive trees* (pp. 31–32). D'Onghia A.M. (ed.), Brunel S.
637 (ed.), Valentini F. (ed.).

638 Chapman, D., White, Steven, Hooftman, Danny A.P., & Bullock, James. (2015). Inventory and
639 review of quantitative models for spread of plant pests for use in pest risk assessment for
640 the EU territory. *EFSA Supporting Publication*, 190.

641 Cornara, D., Bosco, D., & Fereres, A. (2018). *Philaenus spumarius*: When an old acquaintance
642 becomes a new threat to European agriculture. *Journal of Pest Science*, *91*(3), 957–972.
643 <https://doi.org/10.1007/s10340-018-0966-0>

644 Cornara, D., Cavalieri, V., Dongiovanni, C., Altamura, G., Palmisano, F., Bosco, D., Porcelli, F.,
645 Almeida, R. P. P., & Saponari, M. (2017). Transmission of *Xylella fastidiosa* by naturally
646 infected *Philaenus spumarius* (Hemiptera, Aphrophoridae) to different host plants. *Journal*
647 *of Applied Entomology*, *141*(1–2), 80–87. <https://doi.org/10.1111/jen.12365>

648 *Council Directive 2000/29/EC*, (2000). <http://data.europa.eu/eli/dir/2000/29/oj/eng>

649 Cruaud, A., Gonzalez, A.-A., Godefroid, M., Nidelet, S., Streito, J.-C., Thuillier, J.-M., Rossi, J.-P.,
650 Santoni, S., & Rasplus, J.-Y. (2018). Using insects to detect, monitor and predict the
651 distribution of *Xylella fastidiosa*: A case study in Corsica. *Scientific Reports*, *8*(1), 15628.
652 <https://doi.org/10.1038/s41598-018-33957-z>

653 *Decision (EU) 2015/789*, COM (2015). http://data.europa.eu/eli/dec_impl/2015/789/oj/eng

654 *Decision (EU) 2017/2352*, SANTE, COM (2017).
655 http://data.europa.eu/eli/dec_impl/2017/2352/oj/eng

656 Di Serio, F., Bodino, N., Cavalieri, V., Demichelis, S., Di Carolo, M., Dongiovanni, C., Fumarola, G.,
657 Gilioli, G., Guerrieri, E., Paciotti, Ugo, Plazio, E., Porcelli, F., Saladini, M., Salerno, M.,
658 Simonetto, Anna, Tauro, D., Volani, S., Zicca, S., & Bosco, D. (2019). Collection of data and
659 information on biology and control of vectors of *Xylella fastidiosa*. *EFSA Supporting*
660 *Publication*, *EN-1628*, 102. <https://doi.org/10.2903/sp.efsa.2019.EN-1628>

661 EFSA PLH Panel. (2019). Update of the Scientific Opinion on the risks to plant health posed by
662 *Xylella fastidiosa* in the EU territory. *EFSA Journal*, *200*.

663 EFSA PLH Panel. (2020). Update of the *Xylella* spp. Host plant database – systematic literature
664 search up to 30 June 2019. *EFSA Journal*, *61*.

665 EPPO Reporting Service. (2018). *Xylella fastidiosa eradicated from Switzerland* (Fasc. 083).
666 European and Mediterranean Plant Protection Organization.

667 EPPO Reporting Service. (2019). *Xylella fastidiosa subsp. Multiplex was first found in December*
668 *2018 on lavender plants (in a zoo garden) in the municipality of Vila Nova de Gaia (near*
669 *Porto)* (Fasc. 017). European and Mediterranean Plant Protection Organization.

670 REGULATION (EU) 2020/1201, fasc. REGULATION (EU) 2020/1201 (2020). [https://eur-](https://eur-lex.europa.eu/legal-content/EN/TXT/PDF/?uri=CELEX:32020R1201&from=en)
671 [lex.europa.eu/legal-content/EN/TXT/PDF/?uri=CELEX:32020R1201&from=en](https://eur-lex.europa.eu/legal-content/EN/TXT/PDF/?uri=CELEX:32020R1201&from=en)

672 Fierro, A., Liccardo, A., & Porcelli, F. (2019). A lattice model to manage the vector and the infection
673 of the *Xylella fastidiosa* on olive trees. *Scientific Reports*, *9*(1), 8723.
674 <https://doi.org/10.1038/s41598-019-44997-4>

675 Giampetruzzi, A., Morelli, M., Saponari, M., Loconsole, G., Chiumenti, M., Boscia, D., Savino, V. N.,
676 Martelli, G. P., & Saldarelli, P. (2016). Transcriptome profiling of two olive cultivars in
677 response to infection by the CoDiRO strain of *Xylella fastidiosa* subsp. Pauca. *BMC*
678 *Genomics*, *17*, 475. <https://doi.org/10.1186/s12864-016-2833-9>

679 Gyllenberg, M. (2007). Mathematical aspects of physiologically structured populations: The
680 contributions of J. A. J. Metz. *Journal of Biological Dynamics*, *1*(1), 3–44.
681 <https://doi.org/10.1080/17513750601032737>

682 Hopkins, D. L., & Purcell, A. H. (2002). *Xylella fastidiosa*: Cause of Pierce’s Disease of Grapevine and
683 Other Emergent Diseases. *Plant Disease*, *86*(10), 1056–1066.
684 <https://doi.org/10.1094/PDIS.2002.86.10.1056>

685 Ivlev, V. S. (1961). *Experimental ecology of the feeding of fishes*. Yale University Press.

686 Jeger, M., & Bragard, C. (2019). The Epidemiology of *Xylella fastidiosa* ; A Perspective on Current
687 Knowledge and Framework to Investigate Plant Host–Vector–Pathogen Interactions.
688 *Phytopathology*®, *109*(2), 200–209. <https://doi.org/10.1094/PHYTO-07-18-0239-FI>

689 Lopes, J. R. S., Daugherty, M. P., & Almeida, R. P. P. (2009). Context-dependent transmission of a
690 generalist plant pathogen: Host species and pathogen strain mediate insect vector
691 competence. *Entomologia Experimentalis et Applicata*, 131(2), 216–224.
692 <https://doi.org/10.1111/j.1570-7458.2009.00847.x>

693 Montes-Borrego, M., Boscia, Donato, Landa, Blanca B., Saponari, Maria, & Navas-Cortés, J.A.
694 (2017). *Spatial and temporal dynamics of olive quick decline syndrome in orchards in*
695 *Puglia, southern Italy. European Conference on Xylella fastidiosa: Finding answers to a*
696 *global problem*. European conference on Xylella fastidiosa: finding answers to a global
697 problem, Palma de Mallorca.

698 Moralejo, E., Borràs, D., Gomila, M., Montesinos, M., Adrover, F., Juan, A., Nieto, A., Olmo, D.,
699 Seguí, G., & Landa, B. B. (2019). Insights into the epidemiology of Pierce’s disease in
700 vineyards of Mallorca, Spain. *Plant Pathology*, 68(8), 1458–1471.
701 <https://doi.org/10.1111/ppa.13076>

702 Nunney, L., Vickerman, D. B., Bromley, R. E., Russell, S. A., Hartman, J. R., Morano, L. D., &
703 Stouthamer, R. (2013). Recent Evolutionary Radiation and Host Plant Specialization in the
704 *Xylella fastidiosa* Subspecies Native to the United States. *Applied and Environmental*
705 *Microbiology*, 79(7), 2189–2200. <https://doi.org/10.1128/AEM.03208-12>

706 Parnell, S., van den Bosch, F., Gottwald, T., & Gilligan, C. A. (2017). Surveillance to Inform Control
707 of Emerging Plant Diseases: An Epidemiological Perspective. *Annual Review of*
708 *Phytopathology*, 55(1), 591–610. <https://doi.org/10.1146/annurev-phyto-080516-035334>

709 Perring, T., Farrar, C., & Blua, M. (2001). Proximity to citrus influences Pierce’s disease in Temecula
710 Valley vineyards. *California agriculture*, 55(4), 13–18.

711 Purcell, A. H., Saunders, S. R., Hendson, M., Grebus, M. E., & Henry, M. J. (1999). Causal Role of
712 *Xylella fastidiosa* in Oleander Leaf Scorch Disease. *Phytopathology*[®], *89*(1), 53–58.
713 <https://doi.org/10.1094/PHYTO.1999.89.1.53>

714 Redak, R. A., Purcell, A. H., Lopes, J. R. S., Blua, M. J., Mizell III, R. F., & Andersen, P. C. (2004). The
715 biology of xylem fluid-feeding insect vectors of *Xylella fastidiosa* and their relation to
716 disease epidemiology. *Annual Review of Entomology*, *49*(1), 243–270.
717 <https://doi.org/10.1146/annurev.ento.49.061802.123403>

718 Sanderlin, R. S. (2017). Host Specificity of Pecan Strains of *Xylella fastidiosa* subsp. *Multiplex*. *Plant*
719 *Disease*, *101*(5), 744–750. <https://doi.org/10.1094/PDIS-07-16-1005-RE>

720 Saponari, M., Boscia, D., Altamura, G., Loconsole, G., Zicca, S., D’Attoma, G., Morelli, M.,
721 Palmisano, F., Saponari, A., Tavano, D., Savino, V. N., Dongiovanni, C., & Martelli, G. P.
722 (2017). Isolation and pathogenicity of *Xylella fastidiosa* associated to the olive quick decline
723 syndrome in southern Italy. *Scientific Reports*, *7*(1), 17723.
724 <https://doi.org/10.1038/s41598-017-17957-z>

725 Saponari, M., Giampetruzzi, A., Loconsole, G., Boscia, D., & Saldarelli, P. (2019). *Xylella fastidiosa* in
726 Olive in Apulia: Where We Stand. *Phytopathology*[®], *109*(2), 175–186.
727 <https://doi.org/10.1094/PHYTO-08-18-0319-FI>

728 Saponari, M., Loconsole, G., & Nigro, F. (2019). *Knowledge of the pathogenicity and virulence of*
729 *Xylella fastidiosa* subsp. *Pauca* ST53 on susceptible—Deliverable 2.1—H2020 POnTE
730 *project*. [https://www.ponteproject.eu/wp-content/uploads/2019/04/Deliverable-](https://www.ponteproject.eu/wp-content/uploads/2019/04/Deliverable-2.1_Knowledge-of-the-pathogenicity-and-virulence-of-Xylella-fastidiosa-subsp.-pauca-ST53-on-susceptible-hosts_REVREV.pdf)
731 [2.1_Knowledge-of-the-pathogenicity-and-virulence-of-Xylella-fastidiosa-subsp.-pauca-](https://www.ponteproject.eu/wp-content/uploads/2019/04/Deliverable-2.1_Knowledge-of-the-pathogenicity-and-virulence-of-Xylella-fastidiosa-subsp.-pauca-ST53-on-susceptible-hosts_REVREV.pdf)
732 [ST53-on-susceptible-hosts_REVREV.pdf](https://www.ponteproject.eu/wp-content/uploads/2019/04/Deliverable-2.1_Knowledge-of-the-pathogenicity-and-virulence-of-Xylella-fastidiosa-subsp.-pauca-ST53-on-susceptible-hosts_REVREV.pdf)

733 Schneider, K., van der Werf, W., Cendoya, M., Mourits, M., Navas-Cortés, J. A., Vicent, A., & Oude
734 Lansink, A. (2020). Impact of *Xylella fastidiosa* subspecies *pauca* in European olives.

735 *Proceedings of the National Academy of Sciences*, 117(17), 9250–9259.

736 <https://doi.org/10.1073/pnas.1912206117>

737 Sicard, A., Zeilinger, A. R., Vanhove, M., Schartel, T. E., Beal, D. J., Daugherty, M. P., & Almeida, R.

738 P. P. (2018). *Xylella fastidiosa*: Insights into an Emerging Plant Pathogen. *Annual Review of*

739 *Phytopathology*, 56(1), 181–202. <https://doi.org/10.1146/annurev-phyto-080417-045849>

740 Strona, G., Carstens, C. J., & Beck, P. S. A. (2017). Network analysis reveals why *Xylella fastidiosa*

741 will persist in Europe. *Scientific Reports*, 7(1), 71. [https://doi.org/10.1038/s41598-017-](https://doi.org/10.1038/s41598-017-00077-z)

742 00077-z

743 White, S., Bullock, J., Cavers, S., & Chapman, Daniel. (2019). *PHC2018/05—Using modelling to*

744 *investigate the effectiveness of national surveillance monitoring aimed at detecting a*

745 *Xylella fastidiosa outbreak in Scotland* (p. 22). Plnt Health Centre, Scotland’s Centre of

746 Expertise.

747 White, S. M., Bullock, J. M., Hooftman, D. A. P., & Chapman, D. S. (2017). Modelling the spread and

748 control of *Xylella fastidiosa* in the early stages of invasion in Apulia, Italy. *Biological*

749 *Invasions*, 19(6), 1825–1837. <https://doi.org/10.1007/s10530-017-1393-5>

750 White, S. M., Navas-Cortés, J. A., Bullock, J. M., Boscia, D., & Chapman, D. S. (2020). Estimating the

751 epidemiology of emerging *Xylella fastidiosa* outbreaks in olives. *Plant Pathology*,

752 ppa.13238. <https://doi.org/10.1111/ppa.13238>

753

754

Gianni Gilioli: Conceptualization, Formal analysis, Methodology, Software, Writing - Review & Editing, Supervision; **Anna Simonetto**: Conceptualization, Formal analysis, Data Curation, Methodology, Software, Validation, Writing - Original Draft, Review & Editing; **Michele Colturato, Noelia Bazarra, José R. Fernández, Maria Grazia Naso**: Software, Writing - Review & Editing; **Domenico Bosco, Crescenza Dongiovanni, Andrea Maiorano, Olaf Mosbach-Schulz, Juan A. Navas Cortés, Maria Saponari**: Conceptualization, Writing - Review & Editing

Declaration of interests

The authors declare that they have no known competing financial interests or personal relationships that could have appeared to influence the work reported in this paper.

The authors declare the following financial interests/personal relationships which may be considered as potential competing interests:

Maiorano Andrea and Mosbach-Schulz Olaf report a relationship with European Food Safety Authority (EFSA) that includes: employment. The authors Maiorano Andrea and Mosbach-Schulz Olaf write under their own name and the article engages themselves and not the responsibility of EFSA. The views or positions expressed in this publication do not necessarily represent in legal terms the official position of the European Food Safety Authority (EFSA). EFSA assumes no responsibility or liability for any errors or inaccuracies that may appear